

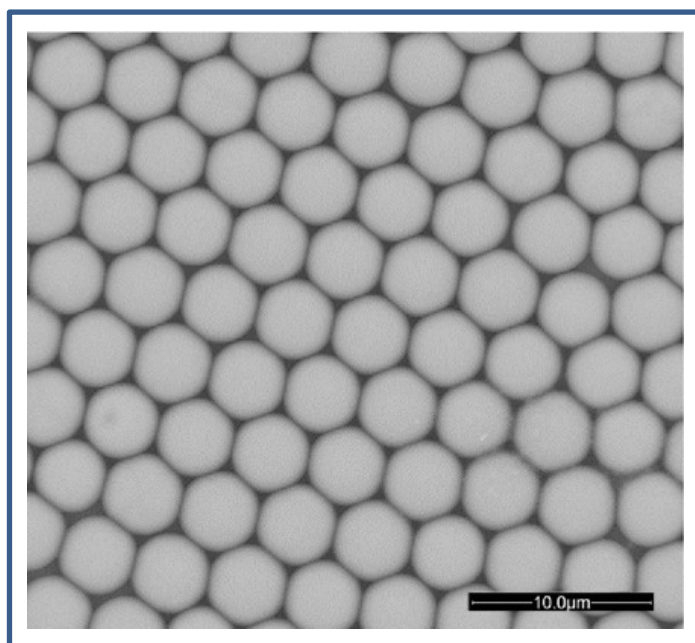


**Published in final edited form as:**

Schmidt, I., & Wagermaier, W. (2017). Tailoring Calcium Carbonate to Serve as Optical Functional Material: Examples from Biology and Materials Science. *Advanced Materials Interfaces*, 4(1): 1600250. doi:10.1002/admi.201600250.

# Tailoring Calcium Carbonate to Serve as Optical Functional Material: Examples from Biology and Materials Science

Ingo Schmidt, Wolfgang Wagermaier



**Basic strategies that manipulate the CaCO<sub>3</sub> material structure of (hemi-)spherical objects** and enable optical functionality are presented. Biological and artificial examples are discussed referring to the structure and the functions of micron sized (hemi-)spherical objects made from CaCO<sub>3</sub>. Birefringence in these examples is eliminated or reduced or this property is even turned into an advantage. Three main approaches were found: manipulation via (i) crystal orientation, (ii) polymorphism, and (iii) crystal size.

## Tailoring calcium carbonate to serve as optical functional material: examples from biology and materials science

*Ingo Schmidt, Wolfgang Wagermaier\**

I. Schmidt, Dr. W. Wagermaier

Max Planck Institute of Colloids and Interfaces, Department of Biomaterials, Potsdam 14424, Germany

E-mail: [wolfgang.wagermaier@mpikg.mpg.de](mailto:wolfgang.wagermaier@mpikg.mpg.de)

Keywords: calcium carbonate, optical functional material, biomineralization, microlenses, birefringence

### Abstract

In nature and technology there are many examples of micron sized optical systems based on minerals. The thermodynamically most stable polymorph of calcium carbonate ( $\text{CaCO}_3$ ) – calcite – exhibits birefringence. However, nature uses biomineralization approaches to produce  $\text{CaCO}_3$  based optical functional materials, for example calcite microlens arrays as part of the photoreceptor system of brittlestars, amorphous  $\text{CaCO}_3$  (ACC) plant cystoliths as light scatterers and calcite trilobite eyes.

In this short review, we illustrate basic strategies to produce optical materials from  $\text{CaCO}_3$  by manipulating the material structure. These strategies are driven by the aim to eliminate or reduce the birefringent properties of calcite, or even, to turn this property into an advantage. We report on the formation, structure, and functions of micron sized (hemi-)spherical objects made from  $\text{CaCO}_3$  with biological origin but also in bio-inspired synthetic examples. We highlight aspects, which pave the way to learn from nature and how to characterize natural and artificial systems.

In conclusion, we identify three main possibilities to make optical materials based on  $\text{CaCO}_3$ : (i) orienting the optical axis along the desired light propagation direction, (ii) stabilizing metastable phases, and (iii) producing nanocrystalline structures, which reduce birefringent properties.

### 1. Introduction

In nature,  $\text{CaCO}_3$ -based biominerals are very common since they consist of simple and easily accessible constituents.<sup>[1]</sup> Some of these biominerals also function as optical devices in organisms.<sup>[2-4]</sup> The most thermodynamically stable form, calcite, would not be an engineer's first choice to produce optical lens systems with one focal point because of the limitations due to birefringence. Biological materials, with and without optical functionality, grow by the principle of self-assembly under ambient conditions and use efficient pathways of inorganic material synthesis.<sup>[5, 6]</sup> The aim of the article is to discuss how nature deals with a birefringent material (calcium carbonate) to use it as optically functional material as well as how this can be achieved in artificial  $\text{CaCO}_3$ -based systems inspired by nature.

The most important polymorphs of  $\text{CaCO}_3$  are ACC, vaterite, aragonite and the most thermodynamically stable form calcite.<sup>[7]</sup> The long-term stability of calcite in neutral environmental conditions enables the use of the material for a variety of technical applications. In general, many crystalline materials show optically anisotropic properties, when –as usual– the atoms are not completely symmetrically arrayed in different crystal lattice directions.<sup>[8]</sup> The crystal lattice of calcite has a rhombohedral symmetry and has a  $R\bar{3}c$  space group (**Figure 1a**). This symmetry can be expressed in a hexagonal setting with the lattice parameters,  $a = 4.98964 \text{ \AA}$ ,  $c = 17.0673 \text{ \AA}$ .<sup>[9]</sup> The crystal symmetry shows an anisotropy in the binding force of the atoms which is also characterized by an anisotropy in the refractive index of the material.<sup>[8]</sup> Calcite is highly birefringent, meaning that the material shows at least two different indices of refraction.<sup>[8]</sup> The carbonate groups are all arranged in planes (see Figure 1a) which are normal to the optical axis.<sup>[8]</sup> The mutual interaction of induced oxygen dipoles differs, when the electronic field vector of the incoming electromagnetic wave is either in or normal to those planes.<sup>[8]</sup> That means, that the light, which does not propagate in direction of the optical axis of the crystal, is split in two light beams due to the optically anisotropy as shown in Figure 1b (yellow arrows  $l_0-l_0'$  and  $l_0-l_1'$ ). In contrast, light passing in the direction of the optical axis (Figure 1b, red arrow  $l_c-l_c'$ ) is not double-refracted and the mineral behaves optically isotropic with a refractive index of 1.486.<sup>[10]</sup> The birefringence of calcite is used in technical applications such as linear polarizers for use with high power lasers.<sup>[8]</sup> The following sections discuss examples from nature and material science where  $\text{CaCO}_3$  is used as optically functional material and where birefringence is not utilized.

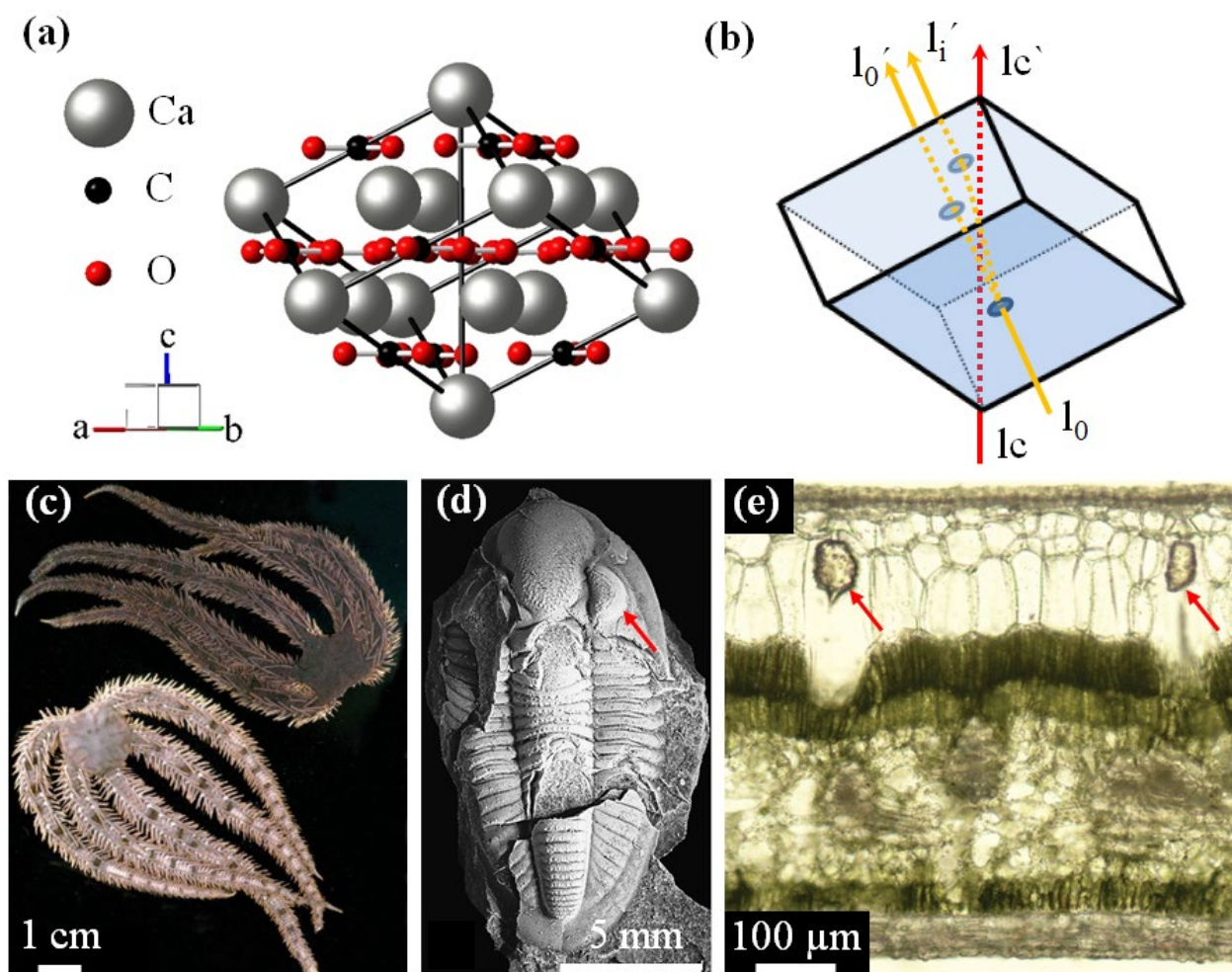


**Figure 1.** a) Calcite crystal structure and b) schematic image of a calcite single crystal oriented the same way as in a). The red arrow  $l_c$ - $l_c'$  in b) shows the path of a light beam in direction of the optical axis of calcite. The yellow arrow  $l_0$  symbolizes an unpolarized light beam which is not parallel to the optical axis of calcite and which is split into two polarized light beams  $l_0'$  (ordinary) and  $l_i'$  (extraordinary) due to a strong birefringent effect of calcite. Panel c) shows the same individual of the brittlestar *Ophiocoma wendtii*, photographed during the day (top) and during the night (bottom). The response to light might be related to the presence of a photoreceptor system containing calcite microlenses. Reproduced from Ref.<sup>[11]</sup> with permission from The Royal Society of Chemistry. An adult trilobite *Paladin eichwaldi shunnerensis* (King, 1914, Middle Carboniferous, Yorkshire, England) with holochroal eyes (region marked with a red arrow) made out of calcite is shown in d).<sup>[12]</sup> A light microscopy image of a fresh, 50  $\mu\text{m}$  thick slice of a *Ficus elastica* leaf is shown in e). The upper epidermis is almost 200  $\mu\text{m}$  thick and the cystoliths marked with red arrows are far from the mesophyll.<sup>[4]</sup>

## 2. Natural optical functional systems

$\text{CaCO}_3$  is a common building block in nature, which enables optical functionality by intricate architectures. The brittlestar *Ophiocoma wendtii* is a prominent example exhibiting microlens

arrays in echinoderms made from calcite single crystals. Figure 1c shows an individual of the brittlestar changing its color depending on the light intensity which the animal detects by its photoreceptor system.<sup>[2]</sup> The oldest preserved visual system of some paleozoic (~542-251 Ma) trilobites like the *Paladin eichwaldi shunnerensis* shown in Figure 1d are based on corneal lenses containing calcite.<sup>[10, 12]</sup> A recent study about the biomineralized armor of the chiton species *Acanthopleura granulata* shows that a visual sensory system includes hundreds of eyes with aragonite-based lenses in the armor.<sup>[13]</sup> The polycrystalline aragonite-based lenses minimize light scattering by the use of relatively large, crystallographically aligned grains.<sup>[13]</sup> These examples of CaCO<sub>3</sub> based materials in animals, as part of photoreceptor systems, have in common that they enable focusing light on visual receptors. Small calcified bodies formed in the leaves of some plants such as *Ficus elasti* (Figure 1e) in the upper epidermis, have a totally different function; they work as light scatterers.<sup>[4]</sup> These amorphous CaCO<sub>3</sub> bodies in a leaf are called cystoliths.<sup>[4]</sup> The following subsections introduce these three natural systems in more detail.

### 2.1. Single crystal calcite microlens arrays in echinoderms

A recent study about calcite microlens arrays embedded in the dorsal arm plates in echinoderms suggest that a complex photoreceptor system in echinoderms had been already acquired in the Late Cretaceous (Campanian and Maastrichtian, ~72.1–66 Ma).<sup>[14]</sup> Fossil echinoderms show a lens-like microstructure on the lateral arm plates and radial shields of Late Cretaceous starfishes and brittlestars.<sup>[14]</sup> The calcite hemisphere structures found in fossils are very similar to the lenses of modern forms.<sup>[14]</sup> Such calcite hemisphere structures within the skeletal construction of the dorsal arm plate have been reported in a few species of modern brittle stars and starfish. For example, a microlens system as part of the photoreceptor system was found on the dorsal arm plate of the brittlestar *Ophiocoma wendtii*,<sup>[2]</sup> as well as comparable structures, which also may be involved in a photoreceptor system of an extant species of the starfish *Archaster typicus*.<sup>[15]</sup> Considering the predator hypothesis, this visual system in echinoderms is part of the adjustment of the animal to its natural habitats.<sup>[16]</sup> The microlenses of the brittlestar *Ophiocoma wendtii* are made from single-crystalline calcite. **Figure 2a** shows a scanning electron microscopy (SEM) image of the microlens array with individual lenses on the surface of the dorsal arm plate. Their unique focusing effect on neural bundles (Figure 2b) with minimized birefringence (Figure 2c) is based on a lens orientation in the direction of the crystallographic *c*-axis of the calcite crystal.<sup>[11]</sup> They are lightweight, mechanically strong, and aberration-free. They display signal enhancement, intensity adjustment, angular selectivity, and photochromic activity.<sup>[11]</sup> These microlenses form an effective optical element that may function as a compound eye unit together with the underlying neural bundles and intraskeletal chromatophores. Aizenberg et al. proposed that these echinoderms are potentially able to extract a considerable amount of visual information about their environment<sup>[17]</sup> by utilizing an orientation approach to prevent the influence of the calcite birefringence on the material function.

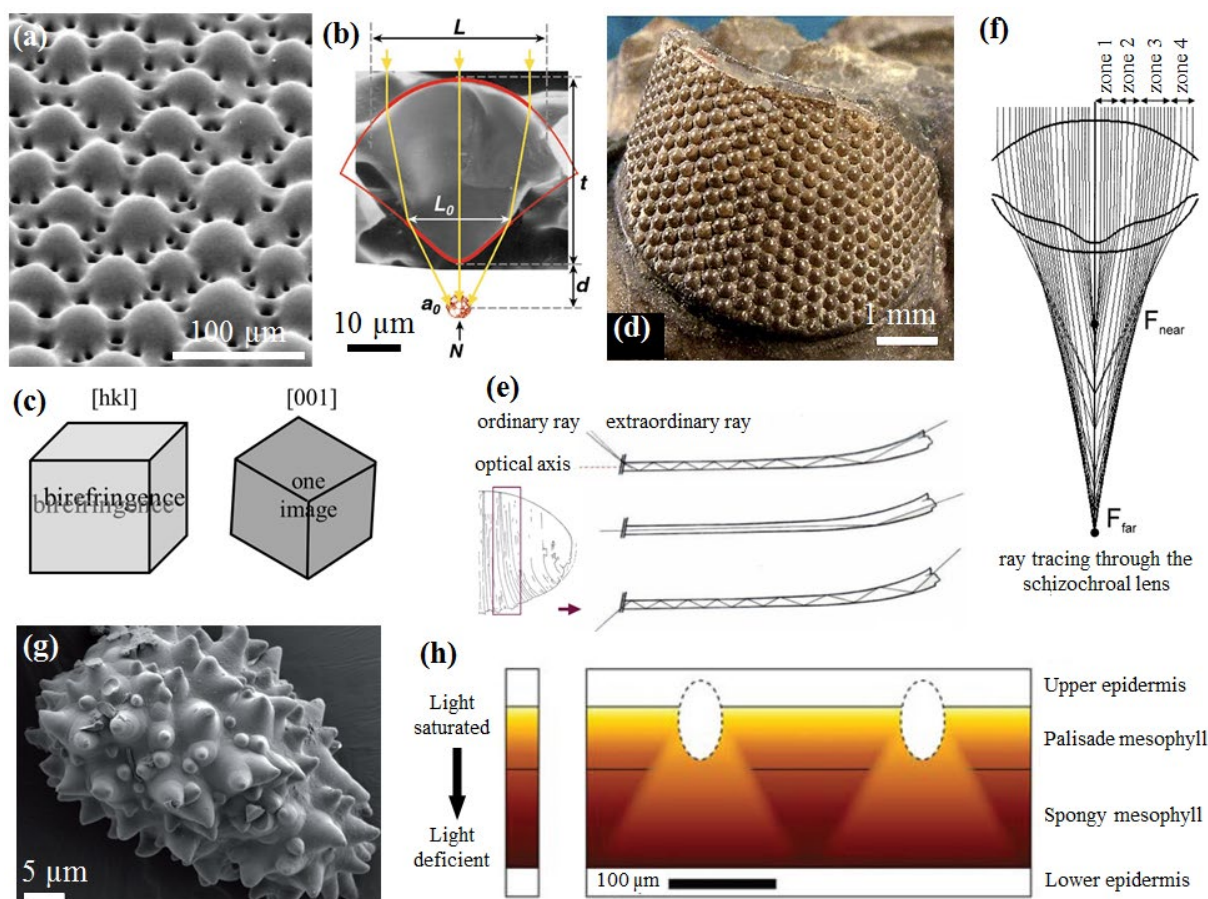


**Figure 2.** a) SEM image of a calcite single crystal microlenses array on the surface of the dorsal arm plate in the brittlestar *O. wendtii* (Reproduced from Ref.<sup>[11]</sup> with permission from The Royal Society of Chemistry) b) SEM image of a cross-section of an individual single crystal lens showing its doublet structure delineated by one spherical and one aspherical surface. Red lines represent the calculated profile of a lens compensated for spherical aberration. The operational part of the calcitic lens ( $L_0$ ) closely matches the profile of the compensated lens (bold red lines). The light paths are shown in yellow. The nerve bundle (N) is shown under the lens (Reproduced from Ref.<sup>[11]</sup> with permission from The Royal Society of Chemistry).<sup>[2, 11]</sup> c) Scheme of the birefringence effect of calcite single crystals. The birefringence can be observed when the crystal is oriented in a general  $\{hkl\}$  crystallographic direction. When the crystal is oriented along the optical axis in the  $[001]$  direction a clear image can be observed. d) Right schizochroal eye of *Hollandops mesocristata* (Le Maitre, 1952, Middle Devonian, Mader, Jbel Issoumour, SE Morocco) with calcite lenses.<sup>[12]</sup> e) Drawing of *Dalmanites sp.* (unknown species and locality) trabecula within lens and light pathway during total internal reflection for the trabeculum shown in the rectangle.<sup>[18]</sup> f) Reconstruction of the change of the back vertex distance of refracted paraxially incident rays of light in the schizochroal doublet lens in *Dalmanitina socialis*. The density of rays was chosen to be greater in those regions of the lens (zones 1, 3) where the back vertex distance is approximately constant. The sharp focusing in zones 1 and 3 and the lack of focusing in zones 2 and 4 could be clearly observed.<sup>[19]</sup> g) SEM image of a *Ficus microcarpa* cystolith, which was extracted from a mature leaf.<sup>[20]</sup> h) "Model drawn to scale of the optical effect of light scatterers in a leaf. The light gradients are highly simplified and only show the relative flux through the tissue and the  $\sim 60^\circ (\pm 30^\circ)$  cone of effective

scattering for each scatterer, under adaxial illumination. Color coded light gradient illustrates the light saturation of the outer mesophyll and the additional light that each scatterer provides to the lower mesophyll below it.”<sup>[4]</sup>

## 2.2. Microcrystalline calcite microlenses in the compound eye of trilobites

The exoskeletons of Paleozoic trilobites preserved as fossil consist of a calcitic-chitinous material.<sup>[10]</sup> The visual organ of some Paleozoic trilobites contains corneal lenses. In 1973, Towe claimed that these lenses were mineralized with calcite while the animals were alive.<sup>[10]</sup> This is supported by subsequent crystallographic research in 2007 by Lee et al..<sup>[21]</sup> Trilobites have two basic types of eyes, simple and compound eyes. The lenses of the simple eyes have its own socket and are grouped together to form a so called schizochroal eye with a hexagonal packing of the circular lenses, which are separated by a thickened cuticular sclera.<sup>[10]</sup> Figure 2d shows the right schizochroal eye of *Hollandops mesocristata*. The corneal parts of the schizochroal eye of *Phacops rana* show radial orientated calcite crystals while the *c*-axis orientation is perpendicular to the external curvature of the lens and the subcorneal lens is crystallographically uniform with a *c*-axis oriented outward through the center of each lens.<sup>[10]</sup> The compound eye consists of closely packed hexagonal prismatic facets or lenses without separations. This architecture is called holochroal eye. For example, the whole holochroal eye of *Isotelus gigas* behaves as each lens of *Phacops rana*, which means, that the crystallographic orientation of calcite is similar.<sup>[10]</sup> Both eye types are made of precisely oriented calcite crystals that show very good optical performances.<sup>[10]</sup> The inner architecture of the lenses of schizochroal and holochroal eyes shows that the lenses consist of fine, orientated microcrystallites, also known as, trabecula (see Figure 2e).<sup>[18]</sup> These trabecula run uninterruptedly throughout the lenses from top to bottom, and are arranged fountainlike. They are vertically ordered in the center of the lens, and more or less fanning out towards the distal lens surface and/or towards the lower surface.<sup>[18]</sup> This arrangement is due to the architecture of the calcitic lenses, in which horizontal organic layers within the lens deposit the calcitic material, forming micro-columns.<sup>[3, 18, 22]</sup> The different refractive indices of the calcite columns ( $n=1.658-1.486$ ) and the embedding organic material ( $n\sim 1.35$ ), implies that each individual trabeculum acts as a light guide, while the whole ‘lens’ acts as a light guiding bundle.<sup>[18]</sup> The lenses of the schizochroal eyed trilobite *Dalmanitina sociales* (see Figure 2f) show an extra feature concerning the optical performance of the calcite lenses. The doublet lenses with a diameter of around 330  $\mu\text{m}$  possess a bulge in each center of the lower surface of the lenses.<sup>[19]</sup> This bulge is associated with bifocal function, since the refractive power of the central region of the lenses (zone 1) is greater than that of the peripheral zone (zone 3). In Figure 2f the zone 1 and 3 of the lens are characterized by relatively sharp focal points  $F_{\text{near}}$  with a smaller focal length and  $F_{\text{far}}$ , while in zone 2 and 4 the back vertex distance changes gradually between  $F_{\text{near}}$  and  $F_{\text{far}}$ .<sup>[19]</sup> The lenses in *Dalmanitina sociales* exhibit this bifocality. The interplay of the calcite crystal orientation and crystal size is represented by oriented microcrystals, which serve as light guiding bundle, eliminates interfering birefringence from the calcite.

### 2.3. Amorphous calcium carbonate plant cystoliths as light scatterers

Oval-shaped bodies of about 60-80  $\mu\text{m}$  in length and 40-60  $\mu\text{m}$  in diameter, known as cystoliths (Figure 2g), are regularly distributed in the epidermis of several angiosperm families, and exhibit common features in different species.<sup>[4, 23]</sup> They protrude into the photosynthetic tissue, the mesophyll.<sup>[4]</sup> The cystolith body is composed of ACC, and is connected by a silicate stalk, which is essential for ACC formation, to the peripheral cell wall.<sup>[4, 20, 24]</sup> In the case of the cystoliths formation of *Ficus elastic* the silicate stalk forms first and is later encapsulated by ACC precipitation. Some species incorporate inorganic ions into the ACC phase of the cystoliths to enhance the stability, but the mechanism of stabilization is still unclear.<sup>[4, 25]</sup> The refractive index of cystoliths is  $1.55 \pm 0.01$ .<sup>[4]</sup> Due to their transparency they function as internal light scatterers that distribute the light flux more evenly inside the leaf.<sup>[4]</sup> A steep light gradient in the leaf is based on the photosynthetic pigments.<sup>[4]</sup> Under most lighting conditions the outer mesophyll is saturated leading to a state where the photosynthetic apparatus is kinetically unable to use the excess light for photochemistry.<sup>[4]</sup> The light scattered by the cystoliths is distributed from the photosynthetically inefficient upper tissue to the more efficient, but light-deprived, lower tissue. This enables the leaf to use the incoming light flux more efficiently.<sup>[4]</sup> The model in Figure 2h shows the area affected by a scatterer using the appropriate anatomical dimensions and scattering angles.<sup>[4]</sup> In this model a distance of  $\sim 200\mu\text{m}$  between scatterers results in an overlapping continuum of scattered light in the lower mesophyll.<sup>[4]</sup> Besides their optical function as light scattering bodies, they may well perform other functions, but these still need to be elucidated.<sup>[4]</sup> The cystoliths are an example for using a stabilized amorphous polymorph to prevent potentially disturbing properties occurring in the long term stable crystal morphologies of  $\text{CaCO}_3$ .

### 3. Artificial calcium carbonate microlens arrays

Optical functional micron sized materials are important for technical applications such as micro-optical devices for light collimating, spreading, and coupling,<sup>[26]</sup> efficiency enhancement in light-emitting devices,<sup>[27]</sup> three-dimensional (3D) imaging,<sup>[28]</sup> single molecule bioimaging,<sup>[29]</sup> and artificial compound eyes.<sup>[30]</sup> Today it is possible to produce optical functional  $\text{CaCO}_3$ -based materials like amorphous, nanocrystalline calcite and calcitic single crystal based microlens arrays as well as highly birefringent vaterite microspheres.<sup>[31]</sup> Often organic additives are used to guide the formation of complex shapes via self-assembly,<sup>[6, 32]</sup> but also without using additives it is possible to get materials with complex shapes.<sup>[33]</sup>

#### 3.1. Amorphous calcium carbonate microlens array

Biocompatible ACC microlens arrays can be synthesized *via* a simple self-assembly route of using a saturated calcium solution, the organic surfactant polysorbate 20, and  $\text{CO}_2$  from air at ambient conditions.<sup>[6]</sup> The formation mechanism is based on a fast self-assembly of nanometer-sized precipitates, mediated by the organic surfactant at the very early stage. A stunted growth with oriented carbonate groups at the edge of the microlenses follows.<sup>[6]</sup> The hexagonally packed lenses are consistent in shape and have uniform size and focal length.<sup>[6]</sup>

**Figure 3a** shows a SEM image of an ACC microlens array. Figure 3b shows the multiple image of a single ‘A’ projected through the array of microlenses. This projection is about  $3.2 \mu\text{m}$ , which is 620 times smaller than the 2 mm object ‘A’. The focal length of about  $7.2 \pm 0.3 \mu\text{m}$  was measured using a confocal microscope as shown in Figure 3c and d. Additionally a focal length of  $8.0 \pm 0.5 \mu\text{m}$  was calculated. The artificial amorphous ACC microlens array represents a strategy to design a birefringence-free optical functional material by using a self-assembly formation mechanism.

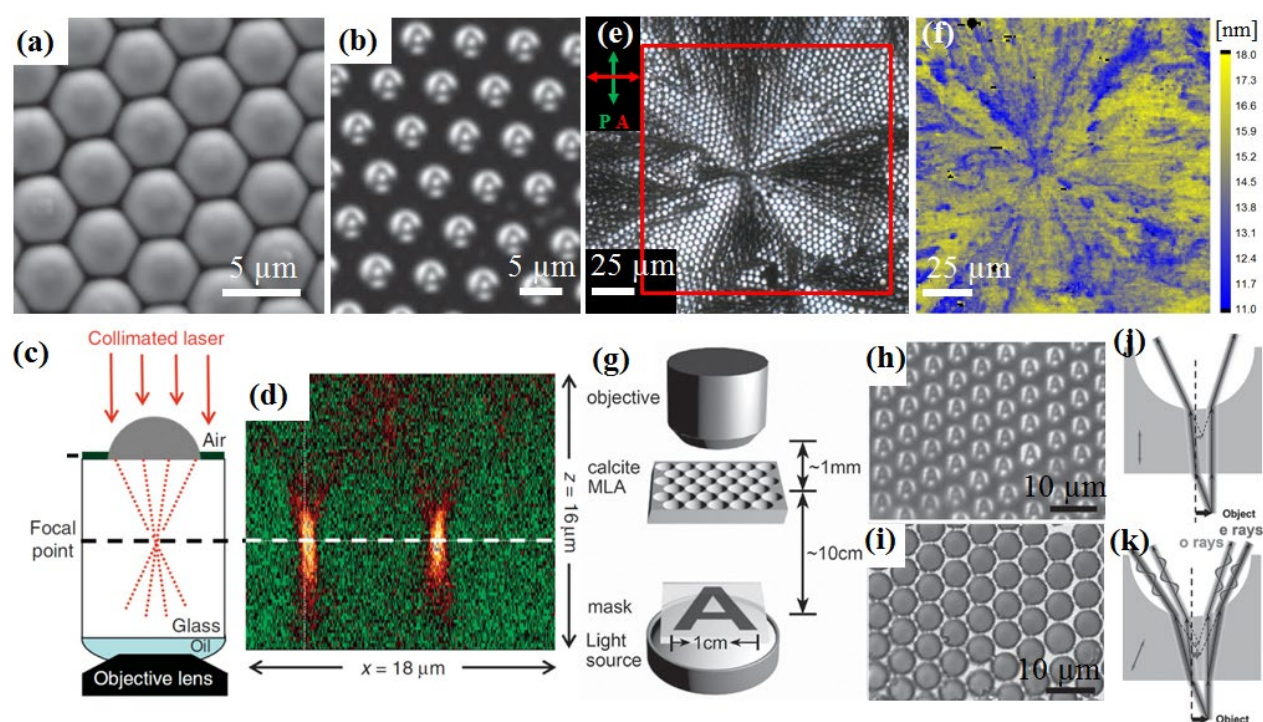


**Figure 3.** a-d)<sup>[6]</sup> show an artificial ACC microlens array. a) SEM image of the well-ordered amorphous  $\text{CaCO}_3$  microlens array (top view). b) optical microscope image of an amorphous  $\text{CaCO}_3$  microlens array and inversely projected ‘A’ array. c) scheme of the confocal microscope with one microlens (grey filled semicircle) on a chitosan-coated (green line) cover glass (white box) and the beam path (red dotted lines) d) focal length characterization of amorphous microlenses using a collimated laser beam ( $650 \pm 10 \text{ nm}$ ).  $x$ - $z$  plane image results from a cross-section taken through a stack of images recorded at different depth in the sample. e-f) the crystallization of the amorphous array results in a nanocrystalline calcite microlens array e) the crystallized microlens array shows a typical spherulite like pattern using polarized optical microscopy.<sup>[34]</sup> f) map of crystallite size in (104) direction measured locally in the red squared region in Figure 3e. g-j)<sup>[35]</sup> artificial concave single crystal calcite microlens array g) schematic setup of the optical system for imaging a centimeter-sized letter ‘A’. h) optical microscope image of calcite (104) microlens array. i) optical microscope images of ‘A’ arrays projected by calcite (104). j) scheme of the optical paths of light propagated through calcite (104) and k) (001) microlens arrays, respectively. The double arrows represent the projected directions of the optical axes of the calcite microlens array.<sup>[35]</sup>

### 3.2. Nanocrystalline calcium carbonate microlens array

For long-term applications it is desirable to transform amorphous materials into the most thermodynamically stable phase.<sup>[36]</sup> The ACC microlens array can be crystallized into stable, nanocrystalline calcite microlens array via thermal heating.<sup>[6, 34, 36]</sup> The microlenses keep their

shape and the array still shows the projected images of 'A' even under cross-polarized light and birefringence.<sup>[6]</sup> The cross-polarized light microscopy image of the calcite microlens array, Figure 3e, shows a spherulite like pattern. This effect is based on a radial propagation of the crystallization front resulting in a radial orientation of the calcite *c*-axis.<sup>[36]</sup> However, calcite is birefringent, which is potentially unfavorable for optical lenses, but the map of the (104) crystallite size (Figure 3f) show that the average size of the differently oriented calcite nanocrystals is about 15-20 nm. The nanocrystalline calcite is based on the minimization of residual strains and the related elastic energy by plastic deformation.<sup>[34]</sup> This effect includes grain boundary formation and twinning of the (001)-type.<sup>[34]</sup> The nanocrystals have a crucial effect on the optical characteristics, because they greatly diminishing the role of the intrinsic birefringence of calcite, and prevent undesirable light scattering at grain boundaries by reducing the system's anisotropy on the wavelength scale.<sup>[36]</sup> The preferred orientation of the optical axes provides some directionality of optical properties.<sup>[36]</sup> The basis of good optical performance of the calcite microlens array is the nanocrystallinity, which is generated by inhomogeneous strains/stresses arising during amorphous/crystalline phase transformation.<sup>[34]</sup> This approach of oriented calcite nanocrystals concatenates the scaling and the orientation approach for producing optically functional calcite materials.

### 3.3. Single crystal based calcium carbonate microlens array

Calcite single crystal concave microlens arrays can be fabricated by template-assisted epitaxial growth in solution without additives under ambient conditions. The crystallographic orientation and the microlens parameters can be adjusted separately by selecting desirable substrates and templates. The optical performance of the artificial microlens arrays was characterized by investigating the microlens' projections of an "A"-symbol as shown in Figure 3g and h. A calcite microlens array with a (001) plane oriented perpendicular to the lens axis showed no birefringence in the direction of the lens axis (Figure 3j). The (001)-calcite microlens array showed an excellent imaging performance like the brittlestar's microlens arrays. A calcite microlens array with a (104) plane oriented perpendicular to the lens axis (Figure 3i) showed birefringent behavior in the direction of the lens axis (Figure 3j). The birefringent calcite (104) microlens array exhibited remarkable polarization-dependent optical properties.<sup>[35]</sup> This calcite single crystal based optically functional material provides a design strategy to use the crystal orientation to create a birefringence-free material as well as to produce a material with birefringence on purpose by using a different crystal orientation.

## 4. Conclusion

Nature provides some intricate strategies to manipulate the material structure for long-term stable  $\text{CaCO}_3$  and to utilize it for optical materials with complex architectures. Today it is possible to design artificial materials inspired by strategies from nature and to eliminate or reduce the birefringent properties of the calcite phase, or to even turn this property into an advantage. The presented examples from nature and the man-made artificial systems show three main possibilities to manipulate  $\text{CaCO}_3$  based systems to enable optical functionality: (i) crystal orientation, (ii) polymorphism and (iii) crystal size. In detail, one can (i) orient the optical axis of a single crystal in a way that it matches the desired function of the system. It is

also possible to (ii) manipulate the formation process by using additives, such as organic molecules or ions, to stabilize metastable material polymorphs with different properties like amorphous or different crystal phases. Another opportunity is to (iii) change the processing of the material to change the crystal size to produce nanocrystalline structures, which reduces birefringent effects. In general, we have summarized strategies to improve current capabilities to fabricate micrometre-scaled optical devices by using easily available materials, and simple but efficient processing inspired by nature.

### Acknowledgements

We want to thank the Max Planck Society for financial support. We also thank Prof. Peter Fratzl, Prof. Emil Zolotoyabko and Dr. Kyubock Lee for scientific discussions as well as Dr. Manfred Burghammer for technical support during the experiments at ESRF.

- [1] a) H. A. Lowenstam, S. Weiner, *On biomineralization*, Oxford University Press, New York, USA **1989**; b) F. Nudelman, N. A. J. M. Sommerdijk, *Angew. Chem. Int. Ed.*, **2012**, 51, 6582.
- [2] J. Aizenberg, A. Tkachenko, S. Weiner, L. Addadi, G. Hendler, *Nature*, **2001**, 412, 819.
- [3] E. N. K. Clarkson, *Palaeontology*, **1979**, 22, 1.
- [4] A. Gal, V. Brumfeld, S. Weiner, L. Addadi, D. Oron, *Adv. Mater.*, **2012**, 24, 77.
- [5] a) P. Fratzl, *J. R. Soc. Interface*, **2007**, 4, 637; b) R. Lakes, *Nature*, **1993**, 361, 511.
- [6] K. Lee, W. Wagermaier, A. Masic, K. P. Kommareddy, M. Bennet, I. Manjubala, S. W. Lee, S. B. Park, H. Colfen, P. Fratzl, *Nat. Commun.*, **2012**, 3, 725.
- [7] H. Colfen, *Curr. Opin. Colloid Interface Sci.*, **2003**, 8, 23.
- [8] E. Hecht, *Optics*, 2<sup>nd</sup> Ed, Addison-Wesley Publishing Co., USA **1990**, pp 282-292.
- [9] E. Zolotoyabko, E. N. Caspi, J. S. Fieramosca, R. B. Von Dreele, F. Marin, G. Mor, L. Addadi, S. Weiner, Y. Politi, *Cryst. Growth Des.*, **2010**, 10, 1207.
- [10] K. M. Towe, *Science*, **1973**, 179, 1007.
- [11] J. Aizenberg, G. Hendler, *J. Mater. Chem.*, **2004**, 14, 2066.
- [12] E. Clarkson, R. Levi-Setti, G. Horváth, *Arthropod Struct. Dev.*, **2006**, 35, 247.
- [13] L. Li, M. J. Connors, M. Kolle, G. T. England, D. I. Speiser, X. H. Xiao, J. Aizenberg, C. Ortiz, *Science*, **2015**, 350, 952.
- [14] P. Gorzelak, M. A. Salamon, R. Lach, M. Loba, B. Ferre, *Nat. Commun.*, **2014**, 5.
- [15] E. Vinogradova, F. Ruíz-Zepeda, G. Plascencia-Villa, M. José-Yacamán, *Zoomorphology* **2015**, 135, 83.
- [16] G. Hendler, *Mar. Ecol.*, **1984**, 5, 379.
- [17] a) J. Aizenberg, D. A. Muller, J. L. Grazul, D. R. Hamann, *Science*, **2003**, 299, 1205; b) S. Yang, C. K. Ullal, E. L. Thomas, G. Chen, J. Aizenberg, *Appl. Phys. Lett.*, **2005**, 86.
- [18] B. Schoenemann, E. N. K. Clarkson, *Earth Environ. Sci. Trans. R. Soc. Edinburgh*, **2011**, 102, 17.
- [19] J. Gal, G. Horvath, E. N. K. Clarkson, O. Haiman, *Vision Res.*, **2000**, 40, 843.
- [20] A. Gal, A. Hirsch, S. Siegel, C. H. Li, B. Aichmayer, Y. Politi, P. Fratzl, S. Weiner, L. Addadi, *Chemistry-a European Journal*, **2012**, 18, 10262.
- [21] M. R. Lee, C. Torney, A. W. Owen, *Palaeontology*, **2007**, 50, 1031.
- [22] a) D. L. Bruton, W. Haas, *Special Papers in Palaeontology*, **2003**, 70, 349; b) J. Miller, E. N. K. Clarkson, *Philos. Trans. R. Soc. B*, **1980**, 288, 461.
- [23] L. Ajello, *Am. J. Bot.*, **1941**, 28, 589.

- [24] H. Setoguchi, M. Okazaki, S. Suga, in *Origin, Evolution, and Modern Aspects of Biomineralization in Plants and Animals*, (Ed: R. Crick), Springer US, **1989**, 409.
- [25] A. Gal, S. Weiner, L. Addadi, *J. Am. Chem. Soc.*, **2010**, 132, 13208.
- [26] N. Ph, R. Völkel, H. P. Herzig, M. Eisner, S. Haselbeck, *Pure Appl. Opt.*, **1997**, 6, 617.
- [27] a) Y. K. Ee, P. Kumnorkaew, R. A. Arif, H. Tong, J. F. Gilchrist, N. Tansu, *Opt. Express*, **2009**, 17, 13747; b) Y. Sun, S. R. Forrest, *Nat. Photonics*, **2008**, 2, 483.
- [28] M. Cho, M. Daneshpanah, I. Moon, B. Javidi, *Proceedings of IEEE Journal*, **2011**, 99, 556.
- [29] J. J. Schwartz, S. Stavrakis, S. R. Quake, *Nat. Nanotechnol.*, **2010**, 5, 127.
- [30] Y. M. Song, Y. Xie, V. Malyarchuk, J. Xiao, I. Jung, K.-J. Choi, Z. Liu, H. Park, C. Lu, R.-H. Kim, R. Li, K. B. Crozier, Y. Huang, J. A. Rogers, *Nature*, **2013**, 497, 95.
- [31] S. J. Parkin, R. Vogel, M. Persson, M. Funk, V. L. Y. Loke, T. A. Nieminen, N. R. Heckenberg, H. Rubinsztein-Dunlop, *Opt. Express.*, **2009**, 17, 21944.
- [32] H. Cao, G. Lin, J. Yao, Z. Shao, *Macromol. Biosci.*, **2013**, 13, 650.
- [33] a) W. L. Noorduin, A. Grinthal, L. Mahadevan, J. Aizenberg, *Science*, **2013**, 340, 832; b) C. Rodriguez-Navarro, K. Kudlacz, O. Cizer, E. Ruiz-Agudo, *CrystEngComm*, **2015**, 17, 58.
- [34] I. Schmidt, E. Zolotoyabko, P. Werner, K. Lee, M. Burghammer, P. Fratzl, W. Wagermaier, *CrystEngComm*, **2015**, 17, 9135.
- [35] X. Ye, F. Zhang, Y. Ma, L. Qi, *Small*, **2014**, 14, 1677.
- [36] I. Schmidt, K. Lee, E. Zolotoyabko, P. Werner, T. S. Shim, Y.-K. Oh, P. Fratzl, W. Wagermaier, *ACS Nano*, **2014**, 8, 9233.